

Response of highly polarized Rydberg states to trains of half-cycle pulses

C. O. Reinhold,^{1,2} W. Zhao,³ J. C. Lancaster,³ F. B. Dunning,³ E. Persson,⁴ D. G. Arbó,⁴ S. Yoshida,⁴ and J. Burgdörfer^{4,2}

¹*Physics Division, Oak Ridge National Laboratory, Oak Ridge, Tennessee 37831-6372, USA*

²*Department of Physics, University of Tennessee, Knoxville, Tennessee 37996-1200, USA*

³*Department of Physics and Astronomy, and the Rice Quantum Institute, Rice University, MS 61, 6100 Main Street, Houston, Texas 77005-1892, USA*

⁴*Institute for Theoretical Physics, Vienna University of Technology, A-1040 Vienna, Austria*

(Received 16 March 2004; published 8 September 2004)

The response of very-high- n strongly polarized potassium Rydberg atoms to a sequence of impulsive perturbations provided by a train of short unidirectional electric pulses is investigated. Each pulse, termed a half-cycle pulse (HCP), has a duration $T_p \ll T_n$, where T_n is the classical electron orbital period. Pronounced differences in the survival probability are observed when the sequence of HCPs is directed parallel and antiparallel to the axis of polarization of the initial state. For impulses directed antiparallel to the initial state, Poincaré surfaces of section point to a mixed phase space with large stable islands embedded in a chaotic sea that can lead to dynamical stabilization. Stable islands are absent when the direction of the impulses is reversed. The system is globally chaotic leading to rapid ionization. We show that noise, i.e., random fluctuations in the temporal pulse-to-pulse spacing as well as in the pulse amplitude, plays a crucial role in the degree of dynamical stabilization. Reasonable agreement between experiment and theory is achieved.

DOI: 10.1103/PhysRevA.70.033402

PACS number(s): 32.80.Rm, 32.80.Qk, 32.60.+i

I. INTRODUCTION

Simple periodically driven systems that are at the borderline between classical and quantum mechanics provide valuable insights into nonlinear dynamics. Prototypes of such systems in atomic physics are the kicked rotor [1–3], Rydberg atoms subject to microwave pulses [4–9], and the kicked Rydberg atom [10–18]. Kicked systems are particularly straightforward to model numerically: their time evolution can be reduced to a sequence of discrete maps between adjacent pulses, which allows detailed analysis of the long-term evolution of the system using both classical and quantum simulations.

The kicked atom has been realized experimentally [12,13] by exposing very-high- n Rydberg atoms to a train of identical equispaced unidirectional electric field pulses, termed half-cycle pulses (HCPs), with durations $T_p \ll T_n$, where T_n is the classical electron orbital period. In this limit each individual HCP, $\vec{F}_{HCP}(t)$, delivers an impulsive momentum transfer or “kick” with strength $\Delta\vec{p} = -\int dt \vec{F}_{HCP}(t)$ to the electron [19]. (Unless otherwise noted, atomic units are used throughout.) The kicked atom furnishes an example of a quantum system whose classical counterpart displays soft chaos, i.e., a mixture of regular and chaotic dynamics. The phase space for the kicked atom contains a series of stable islands enclosed by Kolmogorov-Arnold-Moser tori embedded in a chaotic sea. With an appropriate choice of strength and frequency of the pulse sequence there can be considerable overlap between an initial atomic state and one (or more) of these islands, leading to dynamical stabilization. On the other hand, atoms whose initial states reside in the chaotic sea undergo rapid ionization through diffusion to the continuum.

Many of the theoretical studies of the kicked atom [11–13,15,17,18] have used a one-dimensional (1D) model as it provides a conceptually simple tool to explore various

phenomena observed in three-dimensional (3D) systems. Interestingly, classical and quantum simulations predict that the response of a 1D “atom” will depend critically on the direction of the applied train of HCPs. For kicks directed toward the origin, Poincaré surfaces of section reveal large stable islands indicative of dynamical stabilization. No similar islands are present when the direction of the kicks is reversed. An approximate experimental realization of the 1D model atom has recently become possible using quasi-1D very-high- n atoms created by excitation of selected near-extreme Stark states in the presence of a weak dc field [20–23]. The dynamics of such elongated Stark states when subject to trains of unidirectional pulses is expected to mimic that of its 1D counterpart [12–14]. In the present work, the response of quasi-1D atoms to trains of unipolar HCPs applied along the atomic axis directed either toward or away from the core ion is investigated experimentally and theoretically. Pronounced differences in the survival probability are observed, which point to very different dynamical behavior. The physical origin of this disparate behavior is discussed. We show that such differences can decrease dramatically due to random fluctuations of the train of pulses, i.e., “noise.” This result is consistent with studies of the effect of noise in dynamical stabilization and quantum localization for the kicked rotor [3,24] and Rydberg atoms subject to microwave pulses [25–28].

II. THEORY

In this section we briefly review the basic features of the kicked Rydberg atom (more detailed discussions can be found elsewhere [11–15,17]). The behavior of an atom that is subject to a periodic train of N HCPs with repetition frequency $\nu = 1/T$, where T is the time between adjacent pulses, is governed by the Hamiltonian

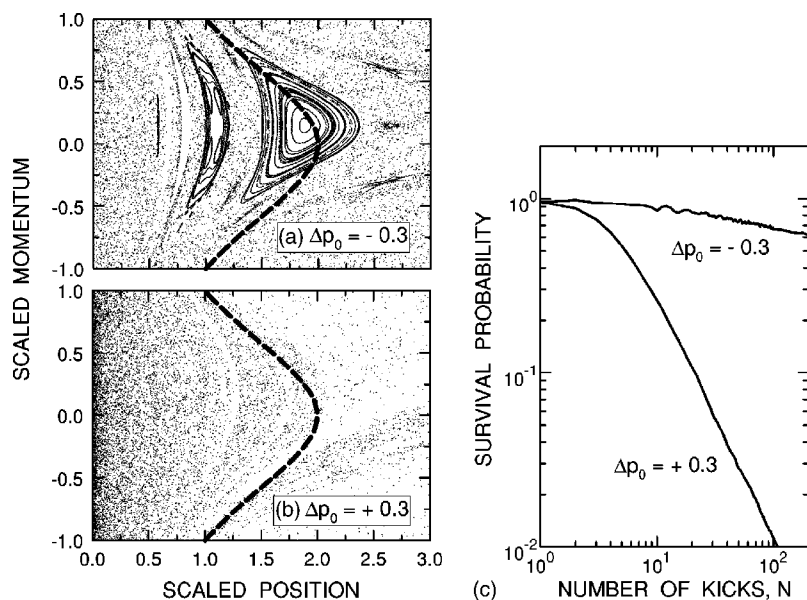


FIG. 1. (a),(b) Poincaré surfaces of section for the 1D kicked hydrogen atom for a scaled frequency of $\nu_0=1.3$ and scaled kick strength $|\Delta p_0|=0.3$. In (a), the kicks are directed toward the origin ($\Delta p_0=-0.3$) and in (b) directed away from the origin ($\Delta p_0=+0.3$). The thick dashed line indicates the unperturbed torus associated with the initial state. (c) Corresponding calculated survival probabilities as a function of the number N of impulses for kicks directed toward and away from the origin.

$$H = \frac{p^2}{2} - \frac{1}{r} + zF(t) \quad (2.1)$$

where $\vec{r}=(x,y,z)$ and $\vec{p}=(p_x,p_y,p_z)$ denote the position and momentum of the electron, respectively. The applied electric field $F(t)$ is given by

$$F(t) = \sum_{k=1}^N F_{HCP}(t-kT) \quad (2.2)$$

where F_{HCP} describes a single half-cycle pulse. In the limit of $\rho=\sqrt{x^2+y^2}\rightarrow 0$ and $p_\rho=(xp_x+yp_y)/\rho\rightarrow 0$, the ρ and z degrees of freedom are only weakly coupled [12,14] and the dynamics along the z direction resembles that described by the 1D Hamiltonian

$$H^{1D} = \frac{p^2}{2} - \frac{1}{q} + qF(t). \quad (2.3)$$

By preparing a highly polarized state with small ρ and p_ρ , the decoupling of the dynamics can be retained for a sizable number of kicks and the limit of a 1D model “atom” can be realized. We note, however, that such decoupling is easier to achieve and maintain when impulses are directed away from the nucleus ($\Delta p > 0$) than when directed toward the nucleus ($\Delta p < 0$). In the limit of a periodic train of ultrashort HCPs (impulses), the field may be written as

$$F(t) = \Delta p \sum_{k=1}^N \delta(t-kT). \quad (2.4)$$

The response of the system to such a train of impulses (“kicks”) can be understood by use of Poincaré surfaces of section. Because the Hamiltonian is periodic in time, Poincaré sections can be generated by taking stroboscopic snapshots of (q,p) during every period of the perturbation. Furthermore, because of classical scaling invariance, the resulting classical phase space portrait will be independent of the initial principal quantum number n when expressed in

terms of the scaled parameters $p_0=pn$, $q_0=q/n^2$, and $T_0=T/(2\pi n^3)$, where the subscript 0 denotes a scaled variable. Deviation from such classical scaling invariance indicates the appearance of quantum effects.

Figures 1(a) and 1(b) show Poincaré surfaces of section for the kicked 1D atom for kicks directed toward ($\Delta p < 0$) and away from ($\Delta p > 0$) the origin, respectively. For $\Delta p < 0$ sizable islands of stability embedded in a chaotic sea are evident. For HCPs with a scaled frequency $\nu_0 \equiv 1/T_0 = 1.3$ the initial state of the electron, denoted by the thick dashed line in Fig. 1(a), overlaps with a large stable island. Those atoms whose initial phase space points lie within the island remain trapped, leading to dynamical stabilization. This is illustrated in Fig. 1(c), which shows the classical survival probability as a function of the number N of kicks. After initially decreasing, the survival probability becomes essentially constant as a result of dynamical stabilization. For dynamical stabilization to occur the electron binding energy must be unchanged following some integer number J of applied kicks. The energy change resulting from a single impulse Δp is given by $\Delta E = (\Delta p)^2/2 + p_i \Delta p$, where p_i is the electron momentum immediately before the impulse. For a period-1 fixed point ($J=1$) this requires that $p_i = -\Delta p/2$, which agrees with the p coordinate of the center of the most prominent island in Fig. 1(a). The impulse then simply reverses the electron momentum to $p_f = \Delta p/2$ without significant change in kinetic energy. Similar dynamical stabilization is also found for other scaled frequencies and is associated with the overlap between the initial state and other islands centered at various periodic orbits with period J . In contrast, for $\Delta p > 0$, the system is globally chaotic and the survival probability decreases monotonically as a function of N for any value of ν_0 [12,18]. Dynamical stabilization does not occur and, as evident from Fig. 1(c), the survival probability falls quite rapidly as N increases.

Analysis of the quantum dynamics of the one-dimensional periodically kicked Rydberg atom has shown that correspondence with the classical behavior depends markedly on the parameters of the train of pulses and on the initial quantum

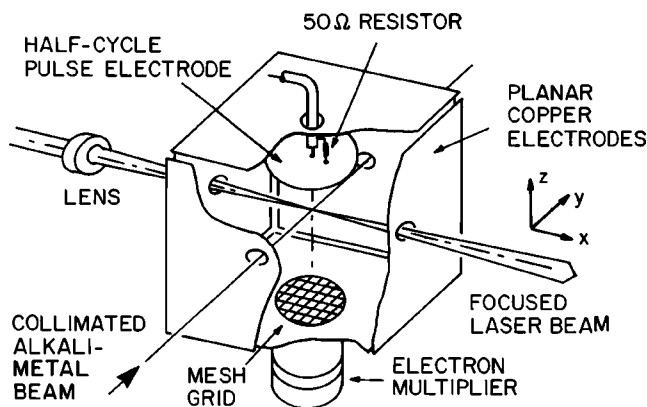


FIG. 2. Schematic diagram of the apparatus.

level of the system. For $\Delta p < 0$ the quantum system is expected to approximately resemble the classical system provided that the size of the stable islands is larger than Planck's constant [17] such as to support quantum states. In turn, classical-quantum correspondence for $\Delta p > 0$ is expected to appear only for large values of the scaled momentum transfer Δp_0 . When the kick strength is small the quantum survival probability as a function of N decreases more slowly than its classical counterpart. This effect is termed quantum localization [14,15] and is, in part, associated with localization around the unstable periodic orbits of the classical system. The behavior of quasi-1D systems as regards to both dynamical stabilization and quantum localization has been found to closely mimic that predicted for 1D systems [12,14]. Because of the additional degrees of freedom the ionization rate (i.e., the chaotic diffusion rate) may be larger in quasi-1D systems than in true 1D systems.

III. EXPERIMENT

To explore the very different predicted behaviors discussed above a series of experiments were undertaken using the apparatus shown schematically in Fig. 2. Quasi-1D high- n atoms are created by photoexciting potassium atoms contained in a thermal-energy beam to select $n=350$ Stark states (eigenstates of the atom in a weak external dc field) using an extracavity doubled frequency-stabilized Coherent CR699-21 Rh6G dye laser. Excitation occurs near the center of an interaction region bounded by three pairs of large copper electrodes. The HCPs are generated by applying voltage pulses to a circular copper electrode mounted on the end of a section of semirigid coaxial cable. This arrangement reduces the stray capacitance of the HCP electrode, allowing fast pulse rise times (≤ 200 ps) to be obtained. Stray fields in the experimental volume can be reduced to $\leq 50 \mu\text{V cm}^{-1}$ by application of small bias potentials to the various electrodes. To create the required Stark states a dc bias field of $\sim 300 \mu\text{V cm}^{-1}$ is established by application of a small bias potential to the HCP electrode. The laser is polarized parallel to the dc field leading to the formation of $m=0$ states. Sizable excitation is observed but only in the vicinity of Stark-shifted s , p , and d levels [20,23], which shows that the oscillator strength is largest in these regions. This finding is

consistent with theoretical predictions [20]. In particular, these calculations indicate that with the laser tuned to the Stark-shifted d level excitation will result in the creation of about 36 low-lying redshifted states in the $n=350$ manifold centered near the parabolic quantum number $n_1 \sim 320$. If the positive z axis is defined to be antiparallel to the applied dc Stark field, the electron probability densities associated with such states are maximal for positive values of z , i.e., the atom is oriented along the $+z$ axis. Their average scaled dipole moment is large, $\langle z \rangle / n^2 \sim 1.25$. These states are thus strongly polarized and form an ideal starting point for studies of quasi-1D atoms.

Experiments are conducted in a pulsed mode. The laser output is formed into a train of pulses of $\sim 1 \mu\text{s}$ duration and 20 kHz repetition frequency using an acousto-optic modulator. (The probability that a Rydberg atom is formed during a single pulse is small and data must be accumulated over many laser pulses.) Immediately following each laser pulse the atoms are subject to a train of HCPs, whose widths and amplitudes are measured using a fast probe and sampling oscilloscope. The number of surviving Rydberg atoms is determined using selective field ionization. For this, a slowly varying positive voltage ramp is applied to the lower-interaction-region electrode. Electrons resulting from field ionization are accelerated to, and detected by, a particle multiplier. Measurements in which no HCPs are applied are interspersed at routine intervals during data acquisition to monitor the number of Rydberg atoms initially created. The Rydberg atom survival probability is then determined by taking the ratio of the Rydberg atom signals observed with and without HCP application.

IV. RESULTS AND DISCUSSION

Figure 3 shows Rydberg atom survival probabilities measured as a function of the number of pulses in the train for a scaled frequency $\nu_0 = 1.3$ and scaled impulses $\Delta p_0 = \pm 0.3$. The scaled width $T_0 = T_p / T_n$ of the 600-ps-wide HCPs used to obtain these data is ~ 0.08 , well within the impulsive limit. Results are included for impulses applied both parallel ($\Delta p > 0$) and antiparallel ($\Delta p < 0$) to the atomic axis. As predicted by the 1D simulations (Fig. 1), the survival probability depends markedly on the direction of the impulses, being typically a factor of 2–3 larger for negative impulses than for positive impulses. Figure 3 also includes results obtained, in the absence of a dc field, using K(351 p) atoms. The measured survival probabilities lie midway between those obtained using quasi-1D atoms. Similar behavior is evident in Fig. 4, which shows the Rydberg atom survival probabilities measured using quasi-1D Stark states and K(351 p) atoms as a function of scaled frequency ν_0 . The peaks in the measured survival probabilities at scaled frequencies $\nu_0 \sim 1.3$ and 0.7 are associated with dynamical stabilization.

Survival probabilities predicted by three-dimensional classical trajectory Monte Carlo (CTMC) simulations are also presented in Fig. 4. Simulations for the time evolution during the train of pulses were performed using a hydrogenic potential as well as a model potential to represent the K^+ core. (We used a model potential that yields accurate quan-

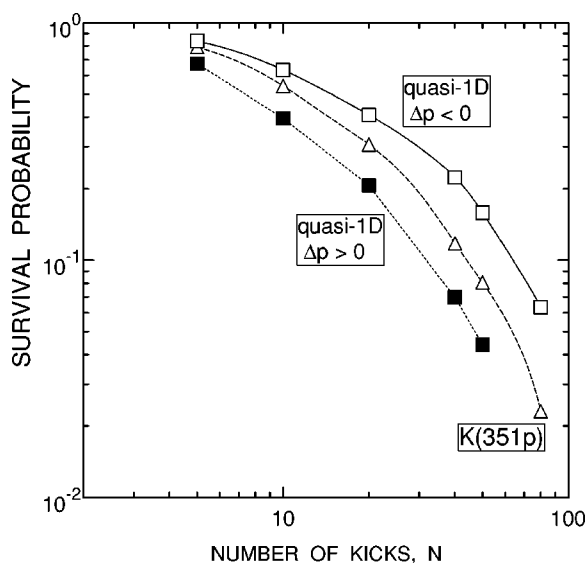


FIG. 3. Measured survival probabilities as a function of the number N of applied HCPs for a scaled frequency $\nu_0=1.3$ and HCPs with a width of 600 ps and a peak field of 170 mV cm^{-1} , which corresponds to a scaled momentum transfer $|\Delta p_0|=0.3$. Results are included for K(351p) atoms (open triangles) and for quasi-1D $n=350$, $m=0$ atoms subject to impulses applied parallel ($\Delta p > 0$) (solid squares) and antiparallel ($\Delta p < 0$) (open squares) to the atomic axis. The lines through the data points are drawn simply to guide the eye.

tum defects and satisfies the correct boundary conditions at small and large distances.) Despite the importance of quantum defects for the photoexcitation process [20,22], no significant changes in the model predictions were noted, indicating that over the time scale of the train of pulses and for high quantum numbers $n \sim 350$ core effects are negligible. Classically, this is due to the fact that the electron stays mostly far away from the core during the time evolution. Note that the angular momentum for $n=351$ precesses rapidly in a wide range $0 < l < 350$ due to the average field associated with the train of pulses, and core effects are important only in the much narrower range $0 < l < 2$. Core effects are also absent during application of each HCP because the rise and fall times are very short and the electronic wave function traverses the Stark map approximately diabatically, following the levels along crossings rather than anticrossings.

In the CTMC calculations the ensemble of points in phase space representing the initial state was propagated in three dimensions according to Hamilton's equation of motion for the Hamiltonian in Eq. (2.1). At the end of the propagation time the final energy E_f of the evolved electron is determined. The overall survival probability is obtained by calculating the fraction of the initial conditions for which $E_f < 0$. (In practice, final states with $n \geq 1200$ will be ionized by the weak dc Stark field but this has only a minor effect on the overall calculated survival probability.) A single experimental HCP profile $F_{HCP}(t)$ was used as the elementary building block in modeling the train of pulses, which was taken to be

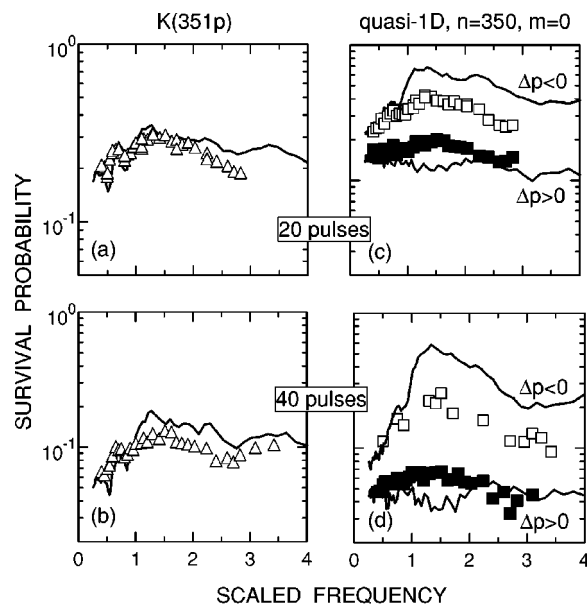


FIG. 4. Survival probabilities as a function of scaled frequency ν_0 for K(351p) atoms (a),(b) and for quasi-1D $n=350$, $m=0$ Stark states subject to impulses applied parallel ($\Delta p > 0$) and antiparallel ($\Delta p < 0$) to the atomic axis (c),(d). The data in (a) and (c) are for $N=20$ impulses while those in (b) and (d) are for $N=40$ impulses. All data correspond to trains of 600-ps-wide HCPs with a peak amplitude of 170 mV cm^{-1} , which yields a scaled momentum transfer $|\Delta p_0|=0.3$. Symbols indicate experimental data. Lines represent CTMC simulations for the anticipated mix of states created by the laser.

$$F(t) \approx \sum_{k=1}^N F_{HCP}(t - T_k). \quad (4.1)$$

For a strictly periodic train of pulses $T_k - T_{k-1} = T$. Measurements revealed one unusual characteristic of the pulse generator used to produce the HCP train in that the time separation between the first and second pulses was systematically about 16% larger than that between subsequent pulses. This is taken into account in the present model calculations by setting $T_2 - T_1 = 1.16T$ and $T_k - T_{k-1} = T$ only for $k > 2$. This unusual characteristic results in a small shift in the positions of the calculated minima and maxima in the survival probability as a function of scaled frequency. The survival probabilities calculated for K(351p) atoms agree reasonably well with experiment. However, the predicted asymmetry for quasi-1D states is larger than that seen experimentally. In particular, the survival probability calculated for negative impulses ($\Delta p < 0$) is much larger than that actually observed. In the following we discuss possible origins of this discrepancy.

In comparing model predictions with experimental data it is necessary to understand precisely which Stark states are being generated by the laser. The calculations in Fig. 4 were performed assuming that laser excitation yields an incoherent mixture of ~ 36 low-lying redshifted states in the $n=350$ manifold centered near the parabolic quantum number $n_1 \sim 320$. This is based on a detailed analysis of the excitation

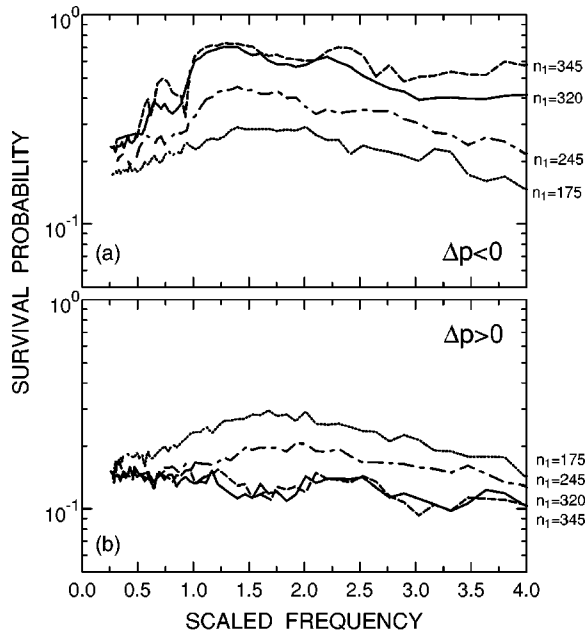


FIG. 5. Predicted survival probabilities as a function of scaled frequency ν_0 for various $K(n=350)$, $m=0$ Stark states with the values of the parabolic quantum number n_1 indicated, following application of $N=20$ impulses directed (a) antiparallel ($\Delta p < 0$) and (b) parallel ($\Delta p > 0$) to the atomic axis. The calculations use a train of pulses that approximately represents the experimental profile but does not include noise. The strength of the impulses is $|\Delta p_0|=0.3$.

process [20] and careful characterization of the product states using multiply directed probe HCPs [23]. Nevertheless, we have investigated the dependence of the survival probability on n_1 using CTMC simulations. Figure 5 displays survival probabilities after $N=20$ pulses as a function of frequency for a variety of initial Stark states with parabolic quantum numbers n_1 ranging from 345 to 175. States with $n_1=345$ lie close to the bottom of the manifold and are strongly quasi-1D, having large scaled permanent dipole moments ~ 1.5 . States with $n_1 \sim 175$ lie close to the center of the manifold and have no significant permanent dipole moment and zero polarization. Each state was modeled by a subset of a micro-canonical distribution with the orientations of the Kepler orbits restricted to that corresponding to the quantum state. Theory predicts sizable differences in the survival probabilities for positive and negative impulses, the size of the asymmetry increasing as n_1 increases, i.e., as the state becomes more quasi-1D.

A reasonable fit to the experimental data can be obtained if it is assumed that states with $n_1 \sim 250$ are being populated. Such states lie close in energy to the center of the s -related peak in the excitation spectrum. To minimize any possible excitation of such states, the laser (which has an effective linewidth of ~ 10 – 12 MHz determined principally by the divergence of the laser and potassium beams) was tuned toward the long-wavelength edge of the d -related peak in the excitation spectrum, under which conditions the Stark-shifted s states lie well outside the bandwidth of the laser. In addition, tests were undertaken in which the laser polarization was set to create $m=1$ states. This suppresses excitation

in the vicinity of the Stark-shifted s level [23] but no systematic differences in the measured survival probabilities were found. This indicates that s -related states are not responsible for the discrepancy between theory and experiment. Furthermore, the discrepancy cannot be attributed to production of high-lying blueshifted states in the neighboring $n=349$ Stark manifold, even though these are oriented along the $-z$ axis and would thus undergo dynamical stabilization when subject to positive ($\Delta p > 0$) impulses. Oscillator strength calculations [20] and the lack of any significant photoexcitation in the corresponding region of the spectrum demonstrate that the likelihood for excitation of such states is very small. The evidence for initial production of quasi-1D states is thus very strong. It should also be noted that the quasi-1D nature of the states is not significantly altered during the interval between excitation and application of the HCP train due to the presence of the weak dc Stark field.

A more likely explanation for the discrepancy between theory and experiment relates to the characterization of the HCP train. Considering that the simulations contain no adjustable parameters, the agreement between the calculated and measured survival probabilities for $K(351p)$ atoms [see Fig. 4(a)] is excellent, especially for $N=20$ pulses. This would suggest that there are no gross errors present in measurements of the HCP train. However, minor fluctuations in the amplitudes and separations of the pulses in the train could have a considerable effect, particularly for a large number of pulses. The presence of such noise is suggested by the fact that the agreement between theory and experiment deteriorates as the number of pulses in the train increases from 20 to 40. Moreover, this tendency is confirmed by Fig. 6(a), which shows the survival probability of $K(351p)$ atoms as a function of the number N of impulses in the train. Analysis of the measured pulse profiles has revealed fluctuations in both the pulse amplitudes and separations of the order of $\pm 5\%$. The actual fluctuations, however, are difficult to observe using a storage scope as this does not display a single HCP train but rather accumulates data over a series of successive HCP trains, which tends to average out fluctuations. To test the possible effects of such fluctuations on the survival probabilities a series of model calculations were undertaken. Rather than using Eq. (4.1), we set

$$F(t) = \sum_{k=1}^N F_{HCP}^k(t), \quad (4.2)$$

with

$$F_{HCP}^k(t) = \lambda_F^k F_{HCP} \left(t - \sum_{i=1}^k \lambda_i^i T_T \right), \quad (4.3)$$

where λ_F^k and λ_i^i represent random fluctuations. Accordingly, the set $\{\lambda_F^k\}_{k \geq 1}$ characterizes amplitude noise while $\{\lambda_i^i\}_{i \geq 1}$ characterizes frequency noise. For a strictly periodic train $\lambda_F^k = \lambda_i^i = 1$.

Figure 6 displays calculations assuming both a “perfect” HCP train [as described by Eq. (4.1)] and “noisy” HCP trains with $\pm 15\%$ uniformly random fluctuations in λ_F^k while maintaining $\lambda_i^i = 1$ and with $\pm 15\%$ uniformly random fluctuations

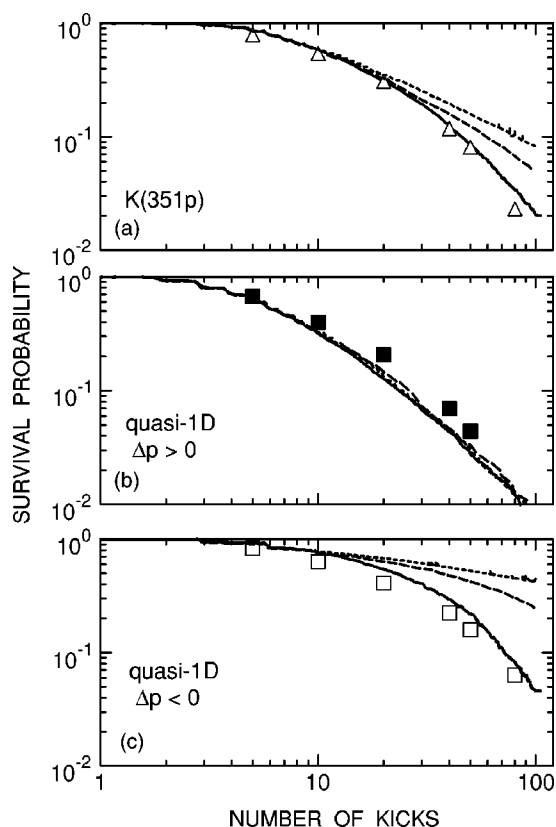


FIG. 6. Comparison of calculated (lines) and measured (symbols) survival probabilities as a function of the number N of impulses for a scaled frequency $\nu_0=1.3$ and a scaled momentum transfer $|\Delta p_0|=0.3$. Results are presented for (a) $K(351p)$ states, and for quasi-1D $n=350$, $m=0$ states subject to impulses applied (b) parallel and (c) antiparallel to the atomic axis. Calculations are presented for deterministic HCP trains with $\lambda_F^k=\lambda_I^k=1$ in Eq. (4.3) (dotted lines), $\pm 15\%$ random fluctuations in the peak amplitudes of the HCPs but $\lambda_I^k=1$ (dashed lines), and $\pm 15\%$ random fluctuations in both the peak amplitudes of the HCPs and the time interval between them (see text).

in both λ_F^k and $\lambda_I^k=1$. The noise amplitude of $\pm 15\%$ was selected in order to obtain reasonable agreement between theory and experiment. In the case of $K(351p)$ atoms [Fig. 6(a)], noise leads to a significant reduction in the predicted survival probability. For quasi-1D atoms and positive impulses [Fig. 6(b)], the introduction of noise in the HCP train leads only to very small changes in the calculated overall survival probability, which is not unexpected given that the system is globally chaotic. The model predictions are in reasonable accord with all the experimental data for $K(351p)$. Note that were a different n_1 distribution assumed, this would not improve the agreement with all the experimental data. The survival probability is most sensitive to noise for quasi-1D atoms and negative impulses [Fig. 6(c)], indicating that the presence of noise leads to the destruction of the stable islands (i.e., noise washes out the stabilization effect brought about by the islands).

In order to investigate whether quantum effects might possibly modify the classical prediction, 3D quantum simulations were also undertaken (Fig. 7). The time-dependent

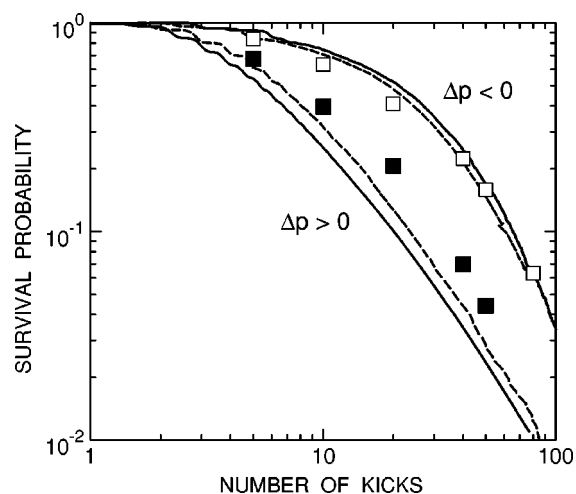


FIG. 7. Comparison of calculated classical (dashed lines) and quantum (solid lines) survival probabilities as a function of the number N of kicks for $\nu_0=1.3$ and $|\Delta p_0|=0.3$ directed parallel ($\Delta p > 0$) and antiparallel ($\Delta p < 0$) to the initial state. The results include $\pm 15\%$ noise in the period and amplitude of the HCPs. The quantum calculations are for a Stark state with quantum numbers $n=50$, $m=0$, $n_1=45$.

Schrödinger equation was solved using the pseudospectral method [29]. This combines a discretization of the radial coordinate optimized for the Coulomb singularity with quadrature methods to allow stable long-time evolution by means of a split-operator approach. The pseudospectral method can be used to simulate the time evolution in the presence of δ function kicks as well as of an arbitrary time-dependent electrical field. We simulate the experimental profile as in the classical calculations. Noise is taken into account by averaging over 400 realizations of the field. Calculations were performed for $n=50$ and $n_1=45$, which gives nearly the same scaled polarization as for $n=350$ and $\langle n_1 \rangle=320$ used in the experiment and the classical calculations. Figure 7 shows that the agreement between the 3D quantum and classical results is quite good, considering that they were performed for very different principal quantum numbers. This strongly suggests that noise (as opposed to nonclassical effects) is responsible for the observed discrepancy between experiment and theory without noise.

V. CONCLUSIONS

The present data demonstrate that the dynamics of quasi-1D atoms subject to a train of kicks depends critically on the direction in which the impulses are applied, the survival probability being much greater when the kicks are directed toward ($\Delta p < 0$) rather than away from ($\Delta p > 0$) the ionic core. For negative impulses the electron is kicked toward the origin where it is backscattered by the Coulomb field of the core, thereby reversing its direction of travel. Under appropriate conditions dynamical stabilization can thus occur, the electron being periodically directed back to the core by the train of applied impulses. No analogous mechanism exists if the electron is kicked away from the

nucleus by positive impulses, which leads simply to chaotic ionization.

Neglecting the possible influence of noise, significant differences between theory and experiment are observed that become increasingly pronounced as the number of kicks increases. Reasonable agreement between theory and experiment can be achieved with both classical and quantum simulations by including $\pm 15\%$ noise in the spacing and strength of the individual HCPs in the train. The data thus show that the dynamics of the kicked Rydberg atom is quite sensitive to the presence of noise in the HCP train. Indeed, kicked atoms should provide an excellent laboratory in which to study the effect of noise on impulsively driven systems. Work is in progress to better characterize the HCP train and

to introduce noise in a controlled fashion, much as in work previously done for microwave-driven Rydberg atoms and kicked cold atoms [3,24–28].

ACKNOWLEDGMENTS

This research was supported by the NSF under Grant No. PHY-0096392 and by the Robert A. Welch Foundation. C.O.R. acknowledges support by the OBES, U.S. DOE under ORNL, which is managed by the UT-Batelle LLC under Contract No. DE-AC05-00OR22725. D.G.A., E.P., S.Y., and J.B. acknowledge support by the SFB 016 ADLIS of the FWF (Austria). J.C.L. also acknowledges support from the Office of Naval Research.

-
- [1] F. L. Moore, J. C. Robinson, C. F. Bharucha, B. Sundaram, and M. G. Raizen, *Phys. Rev. Lett.* **75**, 4598 (1995).
 - [2] B. G. Klappauf, W. H. Oskay, D. A. Steck, and M. G. Raizen, *Phys. Rev. Lett.* **81**, 4044 (1998).
 - [3] V. Milner, D. A. Steck, W. H. Oskay, and M. G. Raizen, *Phys. Rev. E* **61**, 7223 (2000).
 - [4] P. Koch and K. Van Leeuwen, *Phys. Rep.* **255**, 290 (1995).
 - [5] G. Casati, B. V. Chirikov, D. L. Shepelyansky, and I. Guarneri, *Phys. Rep.* **154**, 77 (1987).
 - [6] J. Leopold and D. Richards, *J. Phys. B* **22**, 1931 (1989).
 - [7] A. Buchleitner, D. Delande, and J. Zakrzewski, *Phys. Rep.* **368**, 409 (2002).
 - [8] R. V. Jensen, S. M. Susskind, and M. M. Sanders, *Phys. Rep.* **201**, 1 (1991).
 - [9] M. W. Noel, W. M. Griffith, and T. F. Gallagher, *Phys. Rev. Lett.* **83**, 1747 (1999).
 - [10] R. Blümel and U. Smilansky, *Phys. Rev. A* **30**, 1040 (1984).
 - [11] C. O. Reinhold, J. Burgdörfer, M. T. Frey, and F. B. Dunning, *Phys. Rev. Lett.* **79**, 5226 (1997).
 - [12] M. T. Frey, F. B. Dunning, C. O. Reinhold, S. Yoshida, and J. Burgdörfer, *Phys. Rev. A* **59**, 1434 (1999).
 - [13] B. E. Tannian, C. L. Stokely, F. B. Dunning, C. O. Reinhold, S. Yoshida, and J. Burgdörfer, *Phys. Rev. A* **62**, 043402 (2000).
 - [14] E. Persson, S. Yoshida, X.-M. Tong, C. O. Reinhold, and J. Burgdörfer, *Phys. Rev. A* **68**, 063406 (2003).
 - [15] S. Yoshida, C. O. Reinhold, P. Kristöfel, and J. Burgdörfer, *Phys. Rev. A* **62**, 023408 (2000); S. Yoshida, C. O. Reinhold, and J. Burgdörfer, *Phys. Rev. Lett.* **84**, 2602 (2000).
 - [16] M. Klews and W. Schweizer, *Phys. Rev. A* **64**, 053403 (2001).
 - [17] S. Yoshida, C. O. Reinhold, P. Kristöfel, J. Burgdörfer, S. Watanabe, and F. B. Dunning, *Phys. Rev. A* **59**, R4121 (1999).
 - [18] C. F. Hillermeier, R. Blümel, and U. Smilansky, *Phys. Rev. A* **45**, 3486 (1992).
 - [19] C. O. Reinhold, M. Melles, H. Shao, and J. Burgdörfer, *J. Phys. B* **26**, L659 (1993).
 - [20] C. L. Stokely, J. C. Lancaster, F. B. Dunning, D. G. Arbó, C. O. Reinhold, and J. Burgdörfer, *Phys. Rev. A* **67**, 013403 (2003).
 - [21] T. F. Gallagher, *Rydberg Atoms* (Cambridge University Press, New York 1992).
 - [22] D. G. Arbó, C. O. Reinhold, J. Burgdörfer, A. K. Pattanayak, C. L. Stokely, W. Zhao, J. C. Lancaster, and F. B. Dunning, *Phys. Rev. A* **67**, 063401 (2003).
 - [23] W. Zhao, J. C. Lancaster, F. B. Dunning, C. O. Reinhold, and J. Burgdörfer, *Phys. Rev. A* **69**, 041401 (2004).
 - [24] H. Ammann, R. Gray, I. Shvarchuck, and N. Chistensen, *Phys. Rev. Lett.* **80**, 4111 (1998).
 - [25] L. Sirko, A. Haffmans, M. R. W. Bellermaun, and P. M. Koch, *Europhys. Lett.* **33**, 181 (1996).
 - [26] M. Arndt, A. Buchleitner, R. N. Mantegna, and H. Walther, *Phys. Rev. Lett.* **67**, 2435 (1991).
 - [27] O. Benson, A. Buchleitner, G. Raithe, M. Arndt, R. N. Mantegna, and H. Walther, *Phys. Rev. A* **51**, 4862 (1995).
 - [28] R. Blümel, A. Buchleitner, R. Graham, L. Sirko, U. Smilansky, and H. Walther, *Phys. Rev. A* **44**, 4521 (1991).
 - [29] X.-M. Tong and S. I. Chu, *Chem. Phys.* **217**, 119 (1997); J. Wang, S. I. Chu, and C. Laughlin, *Phys. Rev. A* **50**, 3208 (1994).